Biosensors and Bioelectronics 24 (2008) 994–999

Contents lists available at ScienceDirect

Biosensors and Bioelectronics

journal homepage: www.elsevier.com/locate/bios

Fully reversible optical biosensors for uric acid using oxygen transduction

Petra Schrenkhammer, Otto S. Wolfbeis*

Institute of Analytical Chemistry, Chemo- and Biosensors, University of Regensburg, D-93040 Regensburg, Germany

ARTICLE INFO

Article history:
Received 13 June 2008
Received in revised form 3 August 2008
Accepted 4 August 2008
Available online 13 August 2008

Keywords:
Uric acid
Fluorescence
Oxygen sensor
Oxygen probe
Enzymatic assay

ABSTRACT

An optical biosensor is presented for continuous determination of uric acid. The scheme is based on the measurement of the consumption of oxygen during the oxidation of uric acid that is catalyzed by the enzyme uricase. The enzyme is immobilized in a polyurethane hydrogel next to a metal-organic probe whose fluorescence is quenched by oxygen. The consumption of oxygen was followed by measurement of changes of luminescence intensity of two kind of probes and can be related to the concentration of uric acid. Analytical ranges (0–2 mM), the response times (80–100 s), reproducibility, and long-term stability were investigated. The biosensors are stable for at least 1 month and are not interfered by common interferents. One kind of biosensor was applied to the determination of uric acid in human blood serum. The results agree with those of a commercial colorimetric detection kit.

1. Introduction

The determination of uric acid (UA) plays an important role in clinical medicine. Uric acid (UA) (2,6,8-trihydroxypurine) is the end-product of purine metabolism and excreted by the kidneys and the intestinal tract. The concentration of uric acid in urine of healthy humans is in the millimolar range whereas in blood serum it is in the micromolar range. Abnormally high concentrations of uric acid are symptoms of diseases like gout, hyperuricaemia and the Lesch–Nyhan syndrome (He et al., 2007; Hoshi et al., 2003; Castillo-Ortega et al., 2002; Choi, 2004). Hence, several methods have been developed for the determination of uric acid. Many of them are based on enzymatic oxidation via the enzyme uricase which catalyzes the oxidation of uric acid to give allantoin and hydrogen peroxide (H_2O_2) according to the following equation:

The concentration of uric acid can be determined by measurement of (a) the production of hydrogen peroxide, (b) the consumption of oxygen, or (c) the decrease in the absorbance of uric acid at 293 nm (where allantoin does not absorb). The common method for determination of UA is the uricase method which can be classified in four types the direct equilibrium, the indirect equilibrium, the indirect kinetic, and the direct kinetic uricase methods. The application of the direct equilibrium or kinetic method for UA determination measures the decrease in absorbance of UA at 293 nm. The application of the indirect equilibrium or kinetic method quantifies the amount of H_2O_2 which is produced after completion of the uricase catalyzed oxidation reaction. The various methods for determination of uric acid and the potentially adverse effects of other xanthines on the precision of the methods due to various kinds of enzyme inhibition have been reviewed by Zhao et al. (in press).

Numerous colorimetric methods have been developed for the determination of UA in samples like urine or serum by coupling the uricase reaction to a chromogenic product that is catalyzed by peroxidase and involving H_2O_2 as the oxidant (Fossati et al., 1980; Tamaoku et al., 1982). Based on this approach, an irreversible detection kit has been developed (Haugland, 2002) for fluorometric or spectrophotometric peroxidase-based assays. Other methods for the determination of uric acid are based on voltammetry, amperometry, capillary electrophoresis, or high performance liquid chromatography coupled to detection by either UV absorbance or mass spectroscopy. An irreversible fiber optic biosensor for UA was constructed by immobilizing uricase and horseradish peroxidase (POx) and measuring the hydrogen peroxide produced (Gong and Zhang, 1996; Choi, 2004; Borisov and Wolfbeis, 2008).

Electrochemical methods usually are reversible, while photometric or fluorometric methods based on formation of a chromogenic or fluorescent product are not. Chu et al. (2007) have developed a method that is based on miniaturized capillary electrophoresis with amperometric detection. The group of He et al. (2007) has determined UA in the concentration range from 1 to 50 μM in the presence of ascorbic acid with a quercetin-modified wax-impregnated graphite electrode, and Goyal et al. (2005) have used an electrode modified with fullerene C_{60}.

* Corresponding author. Tel.: +49 941 942 4065; fax: +49 943 941 4064.
E-mail address: otto.wolfbeis@chemie.uni-r.de (O.S. Wolfbeis).

0956-5663/$ – see front matter © 2008 Elsevier B.V. All rights reserved.
doi:10.1016/j.bios.2008.08.007

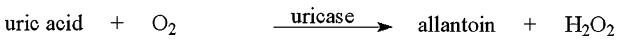

Scheme 1.

A study on a uricase-based biosensor using a glassy carbon electrode modified with Nafion and methyl viologen was reported by Jin et al. (1993). Other recent work includes that of Gutés et al. (2007) have reported on a sequential injection analysis electronic tongue with integrated reference electrode for the simultaneous determination of ascorbic acid, uric acid and paracetamol. Other approaches are based on the use of single-walled carbon nanotube-modified gold electrodes (Wei et al., 2005), of penicillamine self-assembled gold electrodes (Wang et al., 2007; Niu et al., 2007), and of gold electrodes coated with meso-2,3-dimercaptosuccinic acid (Li et al., 2006). Finally, a mesoporus SiO_2-modified carbon paste electrode was reported for the determination of uric acid by Zeng et al. (2008).

We are describing, in this contribution, a sensitive, selective and fully reversible sensing scheme for UA in human blood serum. It is based on a single enzyme/probe sensing layer and exploits the consumption of oxygen as outlined in Scheme 1.

2. Materials and methods

2.1. Materials

Uricase (EC 1.7.3.3), from *Candida* sp. (recombinant, expressed in *Escherichia coli*, lyophilized powder; ≥2 units/mg protein), uric acid, ruthenium(III) chloride hydrate, glutaraldehyde (50 wt% in water) and 3-(trimethylsilyl)-1-propanesulfonic acid sodium salt (purity 97%) were purchased from Sigma–Aldrich (Steinheim, Germany; http://www.sigmaaldrich.com), 3-(*N*-morpholino) propanesulfonate sodium salt (MOPS sodium salt, 98%) from ABCR (Karlsruhe, Germany; http://www.abcr.de), and the Tris(2-phenylpyridyl) iridium(III)complex from Sensient Imaging Technologies GmbH (Wolfen, Germany; http://www.sensient-tech.com). The polyurethane hydrogel Hydromed D4 was obtained from Cardiotech (Wilmington, USA; http://www.cardiotech-inc.com), and the polyester support (Mylar) (product number 124-098-60) from Goodfellow (Bad Nauheim, Germany; http://www.goodfellow.de). The preparation of organically modified sol–gel ("ormosil"), which is soluble in chloroform, was performed as reported before (Klimant et al., 1999). All chemicals and solvents were of analytical grade and were used without further purification. Doubly distilled water was used for the preparation of the 13 mM MOPS buffer solution whose pH was adjusted to 7.5 with 1 M hydrochloric acid.

2.2. Preparation of ruthenium-based oxygen sensitive beads (SB1)

The lipophilic fluorescent oxygen probe $Ru(dpp)_3TMS_2$ was prepared according to the procedure reported by Klimant and Wolfbeis (1995). Then, 400 mg of ormosil beads prepared after Klimant et al. (1999) were dissolved in 50 mL of chloroform, and 7 mg of $Ru(dpp)_3TMS_2$ were added. The resulting "cocktail" was spread onto a glass surface and dried at room temperature. After evaporation of the solvent, the orange colored film was mechanically ground and the resulting particles (of 10–20 μm size) were washed several times with ethanol (in order to remove $Ru(dpp)_3TMS_2$ bound to the surface) until the solution remained colorless. The suspension of SB1 in ethanol was spread onto a glass surface, dried at room temperature, and mechanically ground for a second time. The average size of the beads (SB1) is 5 μm.

2.3. Preparation of iridium-based oxygen sensitive beads (SB2)

Three milligrams of $Ir(ppy)_3$ and 200 mg of ormosil were dissolved in 250 mL of chloroform and the solution was spread on a glass surface. After drying at room temperature, a yellow polymer film was formed, which was ground mechanically. The $Ir(ppy)_3$ beads (referred to as sensor beads SB2) were washed several times by suspending them in ethanol and separating them again by centrifugation. Thereafter, a suspension of SB2 in ethanol was spread onto a glass surface and was dried at ambient air. After evaporation of ethanol, the yellow film was mechanically ground for a second time and treated as described above. The average diameter of the resulting SB2 beads is around 5 μm as determined by microscopy.

2.4. Crosslinking of uricase with glutaraldehyde

Crosslinking of uricase with glutaraldehyde is necessary for formation of a network structure to prevent the leaching of the enzyme out of the sensor membrane. Uricase (20.8 mg) was dissolved in 104 μL of MOPS buffer of pH 7.5 and 26 μL of glutaraldehyde (0.5 wt % in water) was added. The mixture was slightly shaken at room temperature for 2 h. Sensor membranes containing uricase modified in such a way did not suffer from leaching of the enzyme which is in contrast to sensor membranes containing uricase not crosslinked with glutaraldehyde.

2.5. Uric acid biosensor membrane A (BSM1)

Ten milligrams of the beads of type SB1 were dispersed in 500 μL of a 5% weight solution of hydrogel in ethanol/water (9:1, v:v). Then, 130 μL of a MOPS buffered uricase solution with an activity of 100 units (see Section 2.4), crosslinked with glutaraldehyde as described above, was added to the hydrogel, stirred and spread onto the dust-free polyester support by using a self-made knife-coating device. The thickness of the wet sensor layer was 120 μm. After drying at ambient air for 1 h, the resulting sensor layer (referred to as BSM1) was either stored in MOPS buffer or placed in the flow through cell. A cross-section of the membrane is given in Fig. 1.

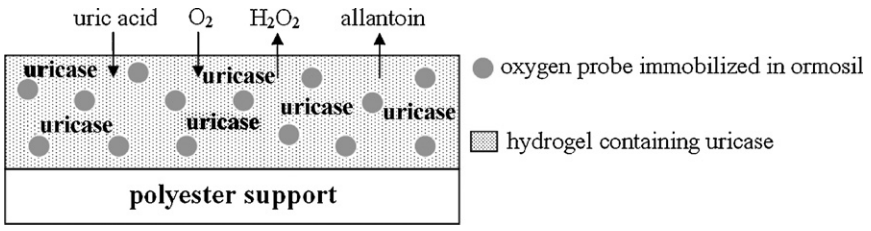

Fig. 1. Cross-section through the biosensor membrane for uric acid, and diffusional processes involved. Uric acid diffuses into the hydrogel membranes while larger (bio)molecules and erythrocytes are kept out. On oxidation of uric acid by the enzyme uricase, oxygen is consumed which is "seen" by the oxygen-sensitive luminescent beads also contained in the hydrogel layer. The thickness of the dried hydrogel layer typically is ~12 μm. The polyester layer is completely inert and only serves as a mechanical – and optically fully transparent – support.

2.6. Uric acid biosensor membrane B (BSM2)

Beads of type SB2 (25 mg) were dispersed in 500 μL of a 5% wt solution of the hydrogel in ethanol/water (9:1, v:v). Then, 130 μL of a MOPS buffered uricase solution with an activity of 100 units (see Section 2.4), crosslinked with glutaraldehyde as described above, was added to the hydrogel, stirred and spread onto a polyester support. The thickness of the wet sensor layer is 120 μm. After drying at room temperature for 1 h, BSM2 was either stored in MOPS buffer or placed in the flow through cell.

2.7. Instrumental

Fluorescence excitation and emission spectra were acquired on an Aminco Bowman AB2 luminescence spectrometer (SLM Spectronic Unicam; http://www.spectronic.co.uk). The luminescence of sensor membrane BSM1 (containing the Ru probe) was excited at 468 nm and emission detected at 612 nm. The luminescence of sensor membrane BSM2 (containing the Ir probe) was excited at 398 nm and emission was detected at 507 nm.

2.8. Measurement of luminescence intensity and lifetime for characterization of BSM1

Response curves for BSM1 were recorded on a phase detection device (PDF-470) from Presens (http://www.presens.de). Light of a 470-nm LED was focused to one branch of a bifurcated glass fiber bundle and directed onto the sensor membrane. Emitted light is guided back by the other branch of the fiber bundle and detected by a photodiode. Luminescence intensity or phase shift detection can be performed simultaneously with this instrument. The excitation light is sinusoidally modulated at a frequency of 49 kHz. The decay time can be calculated from the phase shifts via Eq. (1):

$$\tau = \frac{\tan \rho}{2\pi f} \quad (1)$$

where τ is the decay time, ρ the phase shift, and f is the modulation frequency. Luminescence intensity is proportional to the amplitude of the phase (A) according to Eq. (2),

$$I \propto A^2 \quad (2)$$

A peristaltic pump (Ismatech; http://www.ismatec.de) served to transport solutions from volumetric flasks containing solutions of uric acid in defined concentrations (in buffer) via a tube of 0.25 mm average diameter to the flow-through cell at a flow rate of 0.3 mL per min

2.9. Characterization of BSM2

The response of BSM2 was recorded with a system schematically shown in Fig. S1 in Supplementary part. It consists of an Aminco Bowman AB2 luminescence spectrometer (SLM Spectronic Unicam, http://www.spectronic.co.uk) where the excitation light passed a monochromator and was focused into one branch of a bifurcated glass fiber bundle. The excitation light hits the sensor membrane placed in a self-made flow through cell. The emitted light was guided back by the other branch of the fiber bundle, passed a monochromator and was detected by a photomultiplier. Membrane BSM2 was characterized by passing solutions of uric acid of various concentrations (0–2 mM) through the flow through cell at a rate of 0.7 mL/min. The solutions were transported by a Minipuls-3 peristaltic pump (Gilson, Villiers-le-Bel, France, http://www.gilson.com) via a tube of 0.25 mm diameter.

2.10. Blood serum samples

Human blood serum was sourced from the university hospital of Regensburg. The frozen samples (0.8 mL) were thawed, thermostatted to 22 °C, and diluted with MOPS buffer (pH 7.5) to a volume of 1.4 mL. The calibration curve for determination of UA in serum samples was recorded on a phase detection device (PDD-470) as described in Section 2.8. The amplitude was converted into the intensity according to Eq. (2) in order to make all data comparable. All measurements were performed at 22 ± 1 °C.

3. Results and discussion

3.1. Selection of the luminescent indicators

The $Ru(dpp)_3TMS_2$ probe (whose chemical structure is given in Fig. S2 in Supplementary Part) was selected as the optical oxygen transducer because it has a strong absorption in the visible region of the spectrum (λ_{exc} 468 nm), a large Stokes' shift (λ_{em} 612 nm), a fairly high luminescence quantum yield (~30%) (Cao et al., 2004; Marazuela and Moreno-Bondi, 2002), a long decay time (approximately 4 μs in presence of nitrogen), and can be excited with a blue LED. If trimethylsilylpropane sulfonate is used as the counter ion of the $Ru(dpp)_3$ complex, it is fairly well soluble in the rather lipophilic ormosil (Klimant et al., 1999).

The second indicator used for sensing oxygen [$Ir(ppy)_3$; see Fig. S2 in Supplementary Part] exhibits a broad absorption band with a maximum at 398 nm, and a strong green luminescence (λ_{em}, 507 nm) with a high quantum yield and a long lifetime (<2 μs) (Amao et al., 2001; Amao, 2003). It can be easily immobilized in ormosil due to its lipophilicity. Related iridium probes have been reported recently (Borisov and Klimant, 2007). $Ir(ppy)_3$ is uncharged and well soluble in the ormosil matrix.

3.2. Oxygen sensing capabilities of sensor beads SB1

The uncharged polyurethane hydrogel D4 is an ideal matrix polymer for hosting the oxygen sensitive ormosil beads SB1. It is optically fully transparent, can be easily spread as a thin layer and displays good permeability for oxygen. The luminescence of these sensor beads (ormosil beads of type SB1) incorporated into in a layer of hydrogel is strongly and fully reversibly quenched by oxygen (for a Stern–Volmer plot see Fig. S3 in Supplementary Part). The Stern–Volmer plot is not linear, though. Such situations can be described by a modified equation (Demas et al., 1995) that contains two quenching constants:

$$\frac{I_0}{I} = \left(\frac{f_1}{1 + k_{SV1} \times pO_2} + \frac{f_2}{1 + k_{SV2} \times pO_2} \right)^{-1} \quad (2)$$

Here, I and I_0, respectively, are the quenched and unquenched luminescence intensities of the sensor membrane, k_{SV1} and k_{SV2} are the two Stern–Volmer constants, f_1 and f_2 are the fractions of the total emission for each component, and pO_2 is the partial pressure of oxygen which causes the decrease of the luminescence intensity from I_0 (at pO_2 zero) to I (at $pO_2 > 0$). Eq. (2) is referred to as the two site-model. It reflects the fact that polymer films have two sites of different accessibility for oxygen, each having different quenching constants (Demas et al., 1995; Carraway et al., 1991). The situation is likely to be more complex, but the two-site model is quite adequate to approximately describe the quenching behaviour.

3.3. Oxygen sensing properties of the sensor beads SB2

A Stern–Volmer plot of the quenching by oxygen of the iridium probe incorporated in ormosil beads (SB2) and dispersed in a

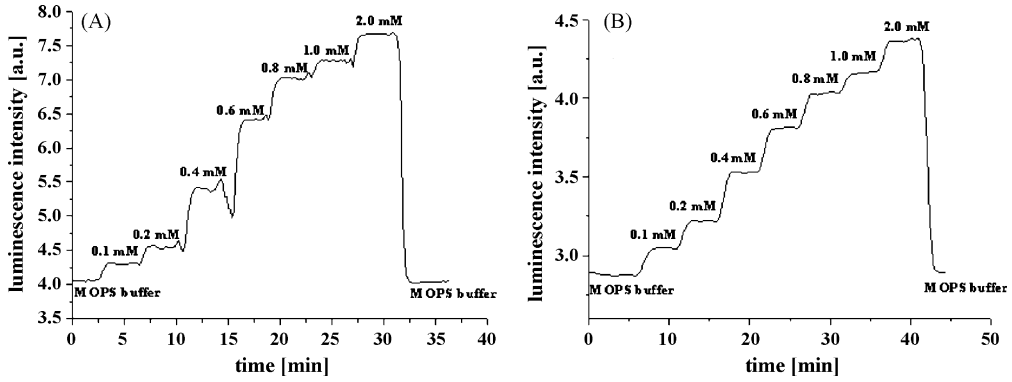

Fig. 2. Relative signal changes, response times, reversibility, and typical dynamic ranges of biosensor membranes BSM1 (A) and BSM2 (B) if exposed to air-saturated solutions of uric acid at a flow rate of 0.3 mL/min.

hydrogel matrix is given in Fig. S3 in Supplementary Part. It follows the conventional Stern–Volmer equation which reads

$$\frac{I_0}{I} = 1 + K_{SV} \times pO_2 \quad (3)$$

where I and I_0, are the quenched and unquenched luminescence intensities of the sensor membrane, and K_{SV} is the Stern–Volmer constant. The data are summarized in Table S1 in Supplementary part.

3.4. Selection of material

The hydrogel D4 has been chosen as the polymer matrix for the sensing membrane due to its good permeability for uric acid and oxygen, its impermeability for charged proteins, its stability, and its optical transparency. It is soluble in a 9:1 ethanol–water mixture and consists of hydrophilic and hydrophobic building blocks which allow the embedding of lipophilic ormosil particles containing the oxygen sensitive dye $Ru(dpp)_3TMS_2$ or $Ir(ppy)_3$ (Schroeder et al., 2005).

The oxygen probes were incorporated into an organically modified sol–gel that is hydrophobic, not penetrated by water in the matrix, but well permeable for oxygen. The material is obtained by acid-catalyzed condensation of phenyl-trimethoxysilane and trimethyl trimethoxysilane in a molar ratio of 18:1. It is soluble in chloroform and acetone, contains much fewer silanol groups than usual ormosils. Consequently, it is less densified over time which enhances the long-term and storage stability of the sensor layer (Klimant et al., 1999; Wolfbeis et al., 2000). Hydrophobic ormosils prevent the penetration of charged species into the matrix and enhance the selectivity for gas sensors.

3.5. Luminescence properties of biosensor membrane BSM1 and BSM2

The excitation and emission spectra, respectively, of the oxygen probes incorporated in ormosil beads are shown in Fig. S4 in Supplementary Part. Beads of type SB1 have an excitation peak at 468 nm so that luminescence can be excited by a 470-nm LED. The red luminescence is peaking at 612 nm. The beads of type SB2 can be excited at around 400 nm, in our case with a purple LED.

3.6. Variation of experimental parameters

The effect of pH on the sensitivity of both biosensor membranes BSM1 and BSM2 were investigated. BSM1 and BSM2 were exposed to a flow of a 1 mM solution of uric acid in buffers of varying pHs (6.5–10.5). The results show that the response is slightly increasing in the pH 6.5–8.0 but then it is stable. A pH of 7.5 was chosen in further experiments. The enzyme uricase was crosslinked with glutaraldehyde in order to prevent leaching of uricase which is the case if it is not crosslinked. Crosslinking was performed at room temperature in buffer of pH 7.5.

3.7. Response of biosensor membranes BSM1 and BSM2

Biosensor membranes BSM1 and BSM2 respond to uric acid in concentrations up to 2.0 mM. Response curves for both biosensors are depicted in Fig. 2A and B. Signal changes can be detected at concentration up to 0.8 mM. There are no useful further signal changes at higher concentrations of UA. The response times are approximately 1.2 min for BSM1, and 1.3 min for BSM2 for a 90% signal change (t_{90}) to occur. The return to the baseline by washing with buffer takes 1.9 min for both sensors. The response times are depending on the enzyme activity and the layer thickness of the sensor membrane. High enzyme activities result in shorter response time. The calculated layer thickness of BSM1 and BSM2 is approximately 12 μm. Thinner membranes could not be manufactured due to the size of the beads which is approximately 5 μm. Layers of thicknesses of less than 12 μm are uneven, whereas thicknesses of 20–25 μm prolong the response times of the sensors, however, without a change in the shape of the calibration graphs (Fig. 3).

3.8. Calibration plots

Fig. 3 shows calibration graphs for membranes BSM1 and BSM2. The signal changes and the dynamic ranges are depending on the enzyme activity in the sensor layer. High uricase activities give larger signal changes. Consequently, the analytical range is narrower compared to low enzyme activities where the analytical range is wider. Best results for both biosensor membranes are obtained with a sensor cocktail (see Sections 2.5 and 2.6) containing uricase with an activity of 100 units. The dynamic range covers around one order of magnitude in each case. The limit of detection (at a signal to noise ratio of 3) is 50 μM for BSM1, and 20 μM for BSM2, obviously a result of the larger quenching constants of probe $Ir(ppy)_3$ (see Table S1 in Supplementary part).

3.9. Stability and reproducibility

The reproducibility of biosensor manufacturing, including the preparation of the sensor beads, is very good in that the calibration curves for the 10 different membranes tested in a row are virtually identical. Biosensor membranes BSM1 and BSM2 are stable for 1 month when stored in MOPS buffer at 4 °C. The response of the

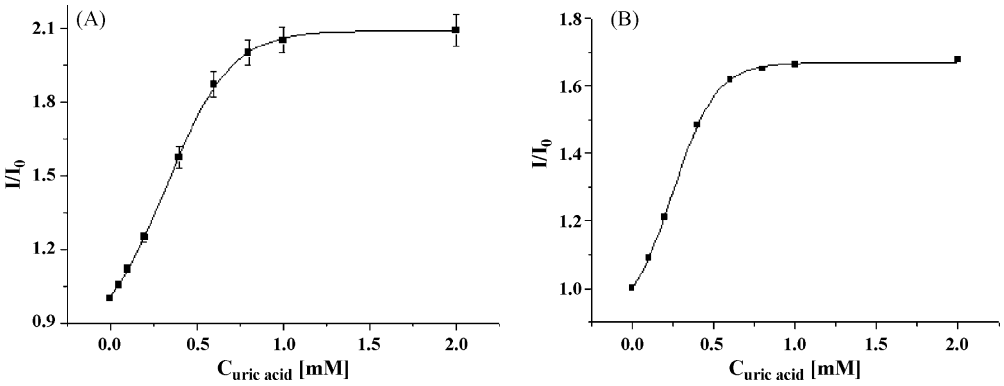

Fig. 3. Dynamic ranges of biosensor membranes BSM1 (A) and BSM2 (B) at pH 7.5. Error bars indicate standard deviations for $n = 5$.

sensor membranes to a 1 mM solution of UA decreases during the first 2 days, probably because enzyme located near the surface is leaching out. Then, the activity remained stable for 3 weeks before activity further decreased.

3.10. Analysis of blood serum samples

Biosensor BSM1 was applied to analyze blood serum samples for UA. UA levels were independently determined by the spectrophotometric method in which UA is converted enzymatically into a purple quinodiime. Frozen serum samples (0.8 mL) were thawed, thermostatted to room temperature and diluted with buffer of pH 7.5 to a volume of 1.4 mL to match the linear range of the calibration plot (Fig. 3A). The membrane BSM1 was first calibrated with standard uric acid solutions ranging from 0 to 2 mM three times before determination of UA in serum samples was carried out. The calibration curve was smoothed via a Boltzmann fit. The UA concentrations were calculated from luminescence intensities using the Boltzmann function. Specified levels and experimental data obtained with the biosensor BSM1 are listed in Table S2 in Supplementary Part.

4. Discussion

The two single-layer optical biosensors presented here for determination of uric acid are simple, sensitive and highly specific. The dynamic range of biosensor membranes BSM1 and for BSM2 is rather wide compared to voltammetric and fluorometric methods (Gong and Zhang, 1996; Martinez-Pérez et al., 2003; Wang et al., 2002). Table 1 summarizes figures of merits of various methods. Most of them exhibit lower LODs. However, the fluorometric methods using Amplex Red or thiamine as substrates require the presence of peroxidase as an additional enzyme in order to convert the non-fluorescent substrates into fluorescent products. The chemiluminescent method using luminol also requires peroxidase.

Further features of the biosensors BSM1 and BSM2 are their applicability at room temperature and at pH 7.5, whereas the chemiluminescent and the fluorometric method using thiamine work best at pH 8.5 (Lv et al., 2002; Gong and Zhang, 1996). The amperometric and the fluorometric methods using thiamine and Amplex Red as substrates are performed at temperatures of >30 °C (Gong and Zhang, 1996; Martinez-Pérez et al., 2003; Luo et al., 2006). Uricase exhibits maximum activity at temperatures between 25 and 37 °C, but we prefer to work at room temperature as its activity was high enough at 22 °C.

The poor selectivity of non-enzymatic voltammetric uric acid biosensors is problematic. Ascorbic acid (AA) heavily interferes as it can be oxidized at the potential applied. To avoid this effect, the electrodes have to be modified for distinct peak assignment of UA and AA (Wang et al., 2002). The sensor beads SB1 and SB2, in contrast, are selective for oxygen. Their signal is not at all disturbed by ascorbic acid, human serum albumin, or cysteine.

Uric acid levels in blood serum are between 120 and 450 μM in healthy subjects (He et al., 2007), while in pathological cases they

Table 1
Overview on uricase-based assays for uric acid

Method	Dynamic range (μM)	LOD (μM)	Remarks
Fluorometry	3–30	0.9	Fiber optic; immobilized UA/POx; based on fluorogenic oxidation of thiamine; irreversible (Gong and Zhang, 1996)
Chemiluminescence	6–600	0.59	Biosensor in a microfluidic system; irreversible (Lv et al., 2002)
Fluorometry	0.02–1	–	Encapsulation of a coupled UA/POx system and Amplex Red in a sol–gel; irreversible (Martinez-Pérez et al., 2003)
Fluorometry	10–1700	25	Sol–gel derived optical array biosensor; stable for 3 weeks; irreversible (Tsai and Doong, 2004)
Spectrophotometry	–	–	Direct kinetic method; based on the measurement of absorbance of uric acid at 293 nm; irreversible (Zhao et al., in press)
Spectrophotometry	–	–	Direct equilibrium method; measurement of absorbance of uric acid at 293 nm; easy calibration on an autoanalyzer; irreversible (Zhao et al., in press)
Voltammetry	5–1000	–	Uricase immobilized on a glassy carbon electrode modified with Nafion and methyl viologen (Jin et al., 1993)
Amperometry	100–800	10	Utilization of a uricase/Ir-C-electrode by using a chronoamperometric method; reversible (Luo et al., 2006)
Potentiometry	4–640	2	Eggshell membrane with UA on an oxygen electrode; response time < 100 s; reversible (Zhang et al., 2007)
Fluorometry	5–600	2	$Ir(ppy)_3$ used as a fluorescent probe for oxygen; t_{90} 1.3 min; reversible (this work)
Fluorometry	5–800	5	$Ru(dpp)_3$ used as a fluorescent probe for oxygen; t_{90} 1.2 min; fully reversible; applicable to whole blood; covers clinical range after dilution and pH adjustment with buffer (this work)

can increase up to 500 μM. For monitoring UA at normal levels in blood serum the samples have to be diluted with buffer which has the addition al advantages that the pH of the sample can be kept adjusted. The results demonstrate that biosensor membrane BSM1 can be applied to blood serum samples. It is the preferred sensor for UA determination because BSM2 suffers from somewhat stronger photobleaching than BSM1. Both sensors membranes display adequate reproducibility (see the error bars in Fig. 3).

The determination of UA in blood serum by the method presented here requires the oxygen concentrations to be constant. As a result, all measurements were performed using air saturated solutions. If oxygen levels vary, a two-sensor approach is required where a first sensor detects the UA level via oxygen consumption as a result of enzymatic oxidation of uric acid, while a second (reference) oxygen sensor is used for determining oxygen of the sample (Wolfbeis et al., 2000). The biosensors BSM1 and BSM2 display stability over 4 weeks. Response times of around 1.5 min, good selectivity and reproducibility in manufacturing of the oxygen sensitive beads and the biosensor membranes are other characteristic features. As it stands now, the dynamic range of the sensor is adjusted to measure UA in diluted serum or blood. If UA is to be measured in undiluted whole blood or serum, the enzyme activity inside the sensor membranes needs to be appropriately reduced. However, pH and oxygen supply need to be kept constant in this case, or need to be determined independently so that their effect can be compensated for.

5. Conclusion

The sensor reported here is capable of both single shot and continuous determination of uric acid in samples such as diluted serum and blood. The optical sensing approach introduced here has distinct advantages over photometric assays in the UV which are not applicable to strongly absorbing solutions, and over electrochemical sensing schemes in terms of selectivity. However, since oxygen consumption is measured, its supply has to be constant, or needs to be determined independently. We believe that this scheme in future may be adapted to the determination of other substrates that can be oxidized with the help of an oxidase.

Acknowledgments

P.S. acknowledges the financial support within the Graduate College GRK 640 (“Photoreceptors in Natural and Artificial Systems”) from the DFG. We thank to Matthias Stich for determination of Stern–Volmer constants and the University Hospital of Regensburg for providing of blood serum samples.

Appendix A. Supplementary data

Supplementary data associated with this article can be found, in the online version, at doi:10.1016/j.bios.2008.08.007.

References

Amao, Y., 2003. Microchim. Acta 143, 1–12.
Amao, Y., Ishikawa, Y., Okura, I., 2001. Anal. Chim. Acta 445, 177–182.
Borisov, S.M., Klimant, I., 2007. Anal. Chem. 79, 7501–7509.
Borisov, S.M., Wolfbeis, O.S., 2008. Chem. Rev. 108, 423–461.
Cao, Y., Koo, Y.E.L., Kopelman, R., 2004. Analyst 129, 745–750.
Carraway, E.R., Demas, J.N., DeGraff, B.A., Bacon, J.R., 1991. Anal. Chem. 63, 337–342.
Castillo-Ortega, M.M., Rodriguez, D.E., Encinas, J.C., Plascencia, M., Méndez-Velarde, F.A., Olayo, R., 2002. Sens. Actuators B: Chem. 85, 19–25.
Choi, M.M.F., 2004. Microchim. Acta 148, 107–132.
Chu, Q.C., Lin, M., Geng, C.H., Ye, J.N., 2007. Chromatographia 65, 179–184.
Demas, J.N., DeGraff, B.A., Xu, W., 1995. Anal. Chem. 67, 1377–1380.
Fossati, P., Prencipe, L., Berti, G., 1980. Clin. Chem. 26, 227–231.
Gong, Z., Zhang, Z., 1996. Anal. Lett. 29, 695–709.
Gutés, A., Calvo, D., Céspedes, F., del Valle, M., 2007. Microchim. Acta 157, 1–6.
Goyal, R.N., Gupta, V.K., Sangal, A., Bachheti, N., 2005. Electroanalysis 17, 2217–2223.
Haugland, R.P., 2002. Handbook of Fluorescent Probes and Research Products 2002, 9th ed.; http://probes.invitrogen.com/handbook/sections/0600.html (viewed in Sep. 2008).
He, J.B., Jin, G.P., Chen, Q.Z., Wang, Y., 2007. Anal. Chim. Acta 585, 337–343.
Hoshi, T., Saiki, H., Anzai, J.I., 2003. Talanta 61, 363–368.
Jin, L., Ye, J., Tong, W., Fang, Y., 1993. Microchim. Acta 112, 71–75.
Klimant, I., Ruckruh, F., Liebsch, G., Stanglmayer, A., Wolfbeis, O.S., 1999. Microchim. Acta 131, 35–46.
Klimant, I., Wolfbeis, O.S., 1995. Anal. Chem. 67, 3160–3166.
Li, N.B., Niu, L.M., Luo, H.Q., 2006. Microchim. Acta 153, 37–44.
Luo, Y.C., Do, J.S., Liu, C.C., 2006. Biosens. Bioelectron. 22, 482–488.
Lv, Y., Zhang, Z., Chen, F., 2002. Analyst 127, 1176–1179.
Martinez-Pérez, D., Ferrer, M.L., Mateo, C.R., 2003. Anal. Biochem. 322, 238–242.
Marazuela, M.D., Moreno-Bondi, M.C., 2002. Anal. Bioanal. Chem. 372, 664–682.
Niu, L.M., Li, N.B., Kang, W.J., 2007. Microchim. Acta 159, 57–63.
Schroeder, C.R., Weidgans, B.M., Klimant, I., 2005. Analyst 130, 907–916.
Tamaoku, K., Ueno, K., Akiura, K., Ohkura, Y., 1982. Chem. Pharm. Bull. 30, 2492–2497.
Tsai, H.C., Doong, R.A., 2004. Anal. Biochem. 334, 183–192.
Wang, L., Bai, J.Y., Huang, P.F., Wang, H.J., Wu, X.W., Zhao, Y.Q., 2007. Microchim. Acta 158, 73–78.
Wang, Z., Wang, Y., Luo, G., 2002. Analyst 127, 1353–1358.
Wei, S., Zhao, F., Zeng, B., 2005. Microchim. Acta 150, 219–224.
Wolfbeis, O.S., Oehme, I., Papkovskaya, N., Klimant, I., 2000. Biosens. Bioelectron. 15, 69–76.
Zeng, Y., Xu, J., Wu, K., 2008. Microchim. Acta 161, 249–253.
Zhang, Y., Wen, G., Zhou, Y., Shuang, S., Dong, C., Choi, M.M.F., 2007. Biosens. Bioelectron. 22, 1791–1797.
Zhao, Y., Yang, X., Lu, W., Liao, H., Liao, F., Microchim. Acta, in press (on-line first doi:101007/s00604-008-0044-z).